

Determination of diffusion coefficient of chloride in concrete: an electrochemical impedance spectroscopic approach

R. Vedalakshmi · R. Renugha Devi · Bosco Emmanuel ·
N. Palaniswamy

Received: 21 February 2007 / Accepted: 30 October 2007 / Published online: 21 November 2007
© RILEM 2007

Abstract For predicting the service life of concrete structures in marine environment, diffusion of chloride (D) is an important parameter. Electro-migration tests and ponding tests are two techniques conventionally adopted, however they are destructive in nature. EIS (Electrochemical impedance spectroscopy) being non-destructive appears a promising technique to arrive at ' D_R ' (D from EIS) in situ in structures. The D_R of ordinary Portland cement concrete (OPC) was compared with that of Portland pozzolana cement concrete (PPC). The effect of curing on D_R was analyzed. The splash zone condition was created by subjecting the specimens to alternate wetting and drying cycles. At the end of 28 days of curing, the D_R of PPC concrete is only 66.7% of that obtained in OPC concrete. A linear correlation was established between D_R and the porosity of the concrete. Due to pozzolanic reaction, the rate of pore refinement is faster in PPC concrete compared to OPC concrete. In M25-PPC concrete at

the end of 28 days of curing, the pore size is decreased to 14.6% of that obtained at the end of 3 days of curing. The reduction of pore size by densification of pore structure due to pozzolanic reaction reduces the D_R value in PPC concrete. In 30 MPa concrete the D_R under wet cycle is 3 times higher than in dry cycle, which implied that corrosion is initiated 3 times faster in concrete exposed to the splash zone condition.

Keywords Diffusion coefficient of chloride · Pore size · Porosity · Resistance · Nernst-Einstein equation

1 Introduction

Chloride-induced corrosion of steel reinforcement is the main cause of deterioration of reinforced concrete structures such as bridges, parking garages, offshore platforms, etc. Seawater and deicing salts used during winter are the sources of chlorides. Corrosion of steel reinforcements leads to concrete fracture through cracking, delamination and spalling of the concrete cover, reduction of concrete and reinforcement cross sections, loss of bond between the reinforcement and concrete, and reduction in strength and ductility. As a result, the safety and serviceability of concrete structures are reduced. Chloride ion permeability is one of the intrinsic properties of concrete to be assessed independently, so as to know the long term

R. Vedalakshmi (✉) · N. Palaniswamy
Corrosion Protection Division, Central Electrochemical
Research Institute, Karaikudi 630 006, Tamilnadu, India
e-mail: corrveda@yahoo.co.in

R. R. Devi
Structural Engineering Department, Thiagarajar College
of Engineering, Madurai 625015, Tamilnadu, India

B. Emmanuel
Modeling and Simulation group, Central Electrochemical
Research Institute, Karaikudi 630 006, Tamilnadu, India



durability and serviceability of concrete structures in marine environment.

For estimation of durability of structures, it is highly desirable to quantify the chloride diffusion process in concrete. When only natural diffusion is involved different conditions/ methods lead to different diffusion coefficients. After concrete has hardened, the diffusion of chloride ions is predominantly controlled by the composition and microstructure of the concrete. Diffusion of chloride is a time dependent process. It will decrease with time since the capillary pore system will be altered as hydration products continue to form. In addition to this, some chloride ions will become chemically or physically bound as they penetrate through the pore system and form complex salts (Friedel's salt). As such it is difficult to precisely predict the diffusion coefficient. It is reported that the short term migration tests give much higher D-values [1]. The most common method widely adopted is the measuring of chloride profile after a predetermined time and fitting this profile in Fick's second law of diffusion. Determination of concentration of chloride by volumetric method is laborious and destructive in nature. A non-destructive method that is applicable in actual field structures needs to be evolved.

Electrochemical Impedance Spectroscopy (EIS) is a potentially useful technique for field-testing of structures. Electrical resistance measurements from EIS represent an additional and fast-developing technique in the study of cement based materials both at micro and macro scale. From the engineering point of view, electrical resistance measurements could be exploited to characterize pore size and diffusion in cement based materials. In predicting the service life of concrete structures, the instantaneous measurement of 'D' in actual concrete structures would prove useful. Advantages of EIS technique over other methods are: (i) The applied AC amplitude is only 20 mV (ii) It takes into account the influences of both bound chloride present in the hydrated cement products as Friedel's salt as well as free chlorides present in the pore solution. (iii) Measurement is easy and quick (iv) The time dependent characteristics of 'D' can be determined.

Xu et al. [2] had observed that the high frequency arc of cement paste in the impedance spectra was inversely proportional to the porosity, pore size and square root of the ionic concentration of the pore

solution. The high frequency arc diameter from EIS measurements can detect real-time micro structural changes in cement paste subjected to a sustained load [3]. It was reported that the increase of the high frequency arc diameter is related to changes in the electrical properties of the C-S-H/pore solution and pore structure parameters induced by the sustained load. The critical chloride concentration for initiation of corrosion has been determined in cement paste from R_p measurements using EIS [4]. A strong decrease in the capacitive part was observed when chloride corrosion initiated on the rebar. The initiation of corrosion was also confirmed by SEM, EDX analysis and visual observation. Buchward et al. [5] carried out studies on masonry materials. Electrical resistance was first determined using EIS technique and converted as conductivity. Using the Nernst-Einstein equation, the diffusion coefficient was arrived at. Diaz et al. [6] established the relation between the diffusion coefficient, resistance from EIS and ionic mobility in cement mortar using four and two electrode methods. McCarter [7] also carried out impedance studies on cement mortars and concluded that the micro structural changes are exerting a more dominant effect on the measured conductivity than changes in pore fluid conductivity.

Thus it can be seen that the earlier studies are mostly confined to cement paste and cement mortar. No detailed studies have been carried out on the efficacy of EIS technique in predicting the chloride diffusion characteristics in concrete. There is also a need to compare the behaviour of pozzolana cement with ordinary Portland cement from the point of view of pore refinement.

The objective of the present investigation is to compare the chloride diffusion characteristics of ordinary Portland cement concrete with that of pozzolana cement concrete under identical curing and testing conditions and predict the durability on the basis of the diffusion coefficients obtained through EIS technique.

2 Experimental method

2.1 Materials

Ordinary Portland cement (OPC)-conforming to BIS1989; equivalent to ASTM type-I cement and



Table 1 Oxide analysis of OPC and PPC

Oxides	Weight (%)	
	OPC	PPC
SiO ₂	20–21	28–30
Al ₂ O ₃	5.2–5.6	7–10
Fe ₂ O ₃	4.4–4.8	4.9–6
CaO	62–63	41–43
MgO	0.5–0.7	1–2
SO ₃	2.4–2.8	2.4–2.8
Loss on ignition	1.5–2.5	3.0–3.5

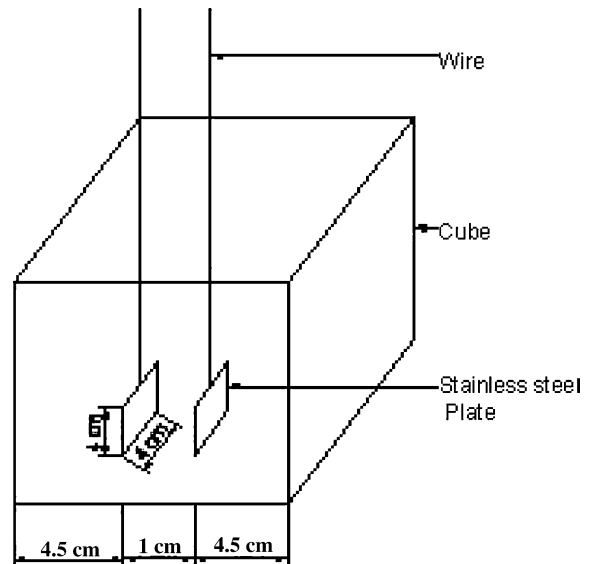
Table 2 Composition of concrete

Grade	Cement (kg/m ³)	Fine aggregate (kg/m ³)	Course aggregate (kg/m ³)	Water (kg/m ³)
M25	284	770	1026	190
M30	352	739	1026	190

Portland pozzolana cement (PPC)-conforming to BIS:1991, have been used in the present investigation. The chemical compositions of the cements are given in Table 1. From the table it can be seen that compared to OPC, the SiO₂ content in PPC is higher whereas the CaO content is lower. Two grades of concrete having a design compressive strength of 25 MPa and 30 MPa were designed as per the procedure outlined in ACI.211-91. The design mixes are given in Table 2. The same proportions have been used for both OPC and PPC concretes. The coarse and fine aggregate conforming to BIS 383:1970 (Specification for coarse and fine aggregate from natural sources for concrete) was used. The maximum size of the aggregate was 20 mm. Potable water was used for casting the concrete. The major difference in the two mixes is the cement content.

2.2 Specimen preparation

As shown in Fig. 1, concrete specimens of size 100 × 100 × 100 mm were cast. In each cube, two number polished stainless steel electrode of size 40 × 40 mm were embedded at 1 cm interval in such a way that they were in perpendicular direction to the diffusion of chloride. Both the top and the bottom

**Fig. 1** Experimental set-up for measuring resistance using Electrochemical impedance spectroscopy

faces of the specimen were sealed with epoxy coating. Electrical leads were taken from the electrodes by brazing and sealed. After demoulding, the specimens were kept immersed in water and cured for different periods viz., 3, 7, 14 and 28 days. The specimens were kept immersed in 0.513 M salt solution for 24 h and then air dried for 6 h at room temperature before EIS experiments were carried out.

2.3 Method of measurement of resistance using EIS

Measurements were carried out in the frequency range 100 kHz–1 Hz using the electrochemical impedance analyser model No. 6310. The amplitude used was 20 mV. The impedance values were plotted in the nyquist plot. Using the software ‘Z view’, the high frequency arc was extrapolated to a semicircle. From the diameter of this semicircle, the resistance of the concrete was calculated and converted into resistivity ‘ ρ ’ using the following equation.

$$\rho = \frac{r \times a}{l} \quad (1)$$

where ρ , resistivity (ohm-m); r , resistance (ohms); a , area of the electrode (m²); l , distance between the driven electrodes (m).

2.4 Diffusion coefficient D_R from resistivity

From the resistance values, the conductivity of the concrete ' σ ' was calculated as follows:

$$\sigma = \frac{1}{\rho} \quad (2)$$

Using the Nernst-Einstein relation [8] the D_R was calculated as:

$$D_R = \frac{RT\sigma}{F^2C} \quad (3)$$

where R, gas constant ($\text{J mol}^{-1} \text{K}^{-1}$); T, temperature (K); F, faraday (C mol^{-1}); C, concentration (mol m^{-3}); σ , conductivity ($\Omega^{-1} \text{m}^{-1}$).

2.5 Alternate wetting and drying cycle

After the impedance measurements, at the end of 28 days curing, were completed, the specimens were subjected to alternate wetting in 3% NaCl solution (0.513 M) for 4 days and drying at 70°C for 3 days to simulate the splash zone condition of the structure. At the end of each wet and dry cycle, impedance measurements were repeated. The impedance plot of M25 & M30 concrete under wet and dry cycle is given in Fig. 7. The experiment was conducted over a period of 64 days.

2.6 Determination of porosity

The porosity of the concrete was determined by the oven drying method given in ASTM C642-90 [9]. For this test, 80 mm diameter and 40 mm thick concrete disks were cast and cured for different periods viz., 3, 7, 14 and 28 days. The specimens were dried in an oven at a temperature of $100 \pm 5^\circ\text{C}$ for 48 h and allowed to cool to room temperature. The weight of the oven-dried specimen (A) was measured. Then the specimen was kept immersed in water continuously for 48 h and after wiping out the surface moisture, the increase in weight (B) was measured. The specimen was then kept immersed in boiled water continuously for a period of 5 h and its weight (C) was taken after a time gap of 14 h. The specimen was suspended in water and its submerged weight (D) was determined.

To determine the % of total voids, apparent specific gravity of the specimen (g_3) has to be determined. The specimen was broken, crushed and powdered for this purpose. 64 grams of powdered sample were taken after sieving through a 90 μ sieve. As per the procedure outlined in IS: 4031, the specific gravity of the powdered sample was determined using a Le-chatelier flask [10].

$$\% \text{ of total voids} = \frac{(g_3 - g_1)}{g_3} \times 100$$

where, $g_1 = A/(C - D)$; A, weight of oven dried sample in air; C, saturated weight of surface dry sample in air after immersion in water; D, submerged weight in water; g_3 , apparent specific gravity of the specimens.

$$\text{Porosity, \%} = \frac{\text{Void volume of concrete}}{\text{Total volume of concrete}} \times 100 \quad (4)$$

2.7 Determination of $D_c(x)$ using chloride concentration (destructive method)

The chloride concentration was determined by volumetric analysis using the silver nitrate method [11]. After the exposure of concrete specimens in chloride solution for 64 days, the chloride concentration at 10 and 20 mm depth was determined. Specimens were sliced at 10 and 20 mm depth, then powdered and sieved through a 300- μm sieve. 30 grams of powdered sample was taken, dissolved in 60 ml of distilled water and left for 24 h to allow for complete dissolution of water-soluble chlorides. After 24 h, the decanted solution was filtered and 5 ml of this filtered solution was neutralized with 0.1 N H_2SO_4 using phenolphthalein as an indicator. Then the solution was titrated against 0.01 N silver nitrate using potassium chromate as an indicator. Yellow to brick red was taken as the end point of the titration. The titrated value was expressed as chloride concentration (C_x). According to Fick's Rule, the diffusion coefficient of concrete can be calculated using the following formula [12],

$$C_x = C_s \left(1 - \operatorname{erf} \left[\frac{x}{2\sqrt{D_{\text{app}}t}} \right] \right) \quad (5)$$

where, C_x , chloride concentration at known depth; C_s , surface chloride concentration (mol/cm^3); x, cover in



concrete (cm); D_{app} , apparent diffusion coefficient (cm^2/s); t , period of exposure(s); The $D_c(x)$ depends upon the porosity and tortuosity of the concrete. It is obtained from D_{app} as follows:

$$D_c(x) = \frac{D_{app} \times \tau}{P} \tag{6}$$

where, τ , tortuosity; P , porosity.

Maekawa et al. reported [13] that the tortuosity factor of concrete varied from 2 to 4 if the microstructure of the concrete varied from coarse to dense. As M25 and M30 concrete mixes used in the present studies are moderately dense (density is around 2300 kg/m^3), a tortuosity value of 3 is appropriate.

3 Results

3.1 D_R from impedance study

Figures 2 and 3 show the impedance plots for M25 and M30 OPC- concrete whereas Figs. 4 and 5 show the impedance plots of M25 and M30 PPC concrete. It can be seen that invariably, in all the plots, two arcs are visible; one at the high frequency region between 100 kHz and 100 Hz and another one at the low frequency region between 100 Hz and 10 Hz. The former is attributed to the solid hydrated cement products and pore solution whereas the latter is attributed to the cement- electrode interface. The

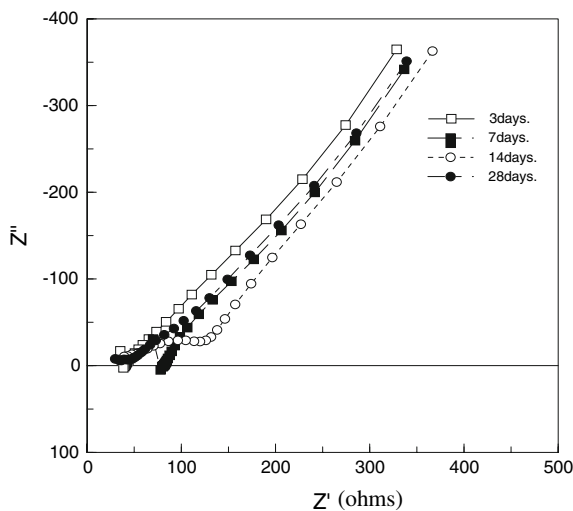


Fig. 2 Impedance data obtained on M25 concrete using OPC

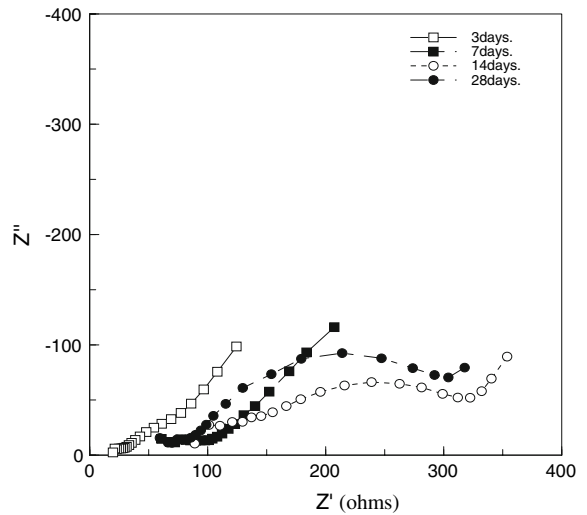


Fig. 3 Impedance data obtained on M30 concrete using OPC

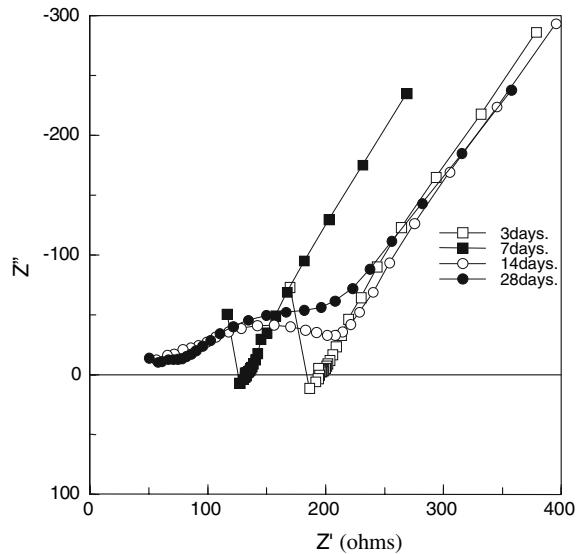


Fig. 4 Impedance data obtained on M25 concrete using PPC

equivalent circuit model, which takes into account the presence of two time constants (Fig. 6).

The diameter of the high frequency arc is taken as the bulk resistance of the concrete. Bulk resistance is inclusive of resistance offered by solid phases present in the concrete and free ions in the pore solution. In both OPC and PPC concretes at the end of 3 days curing, the high frequency arc is not visible. However the high frequency arc appears after 7 days and continues to grow in diameter with time. The high ionic concentrations and high initial porosity delayed

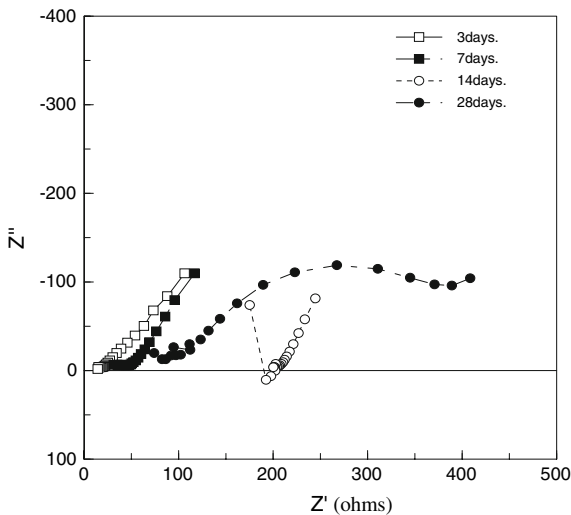


Fig. 5 Impedance data obtained on M30 concrete using PPC

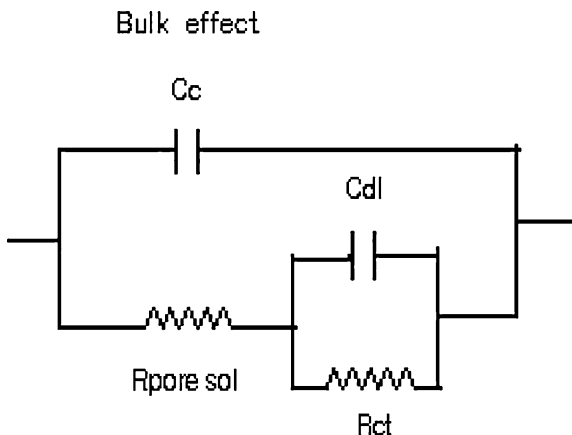


Fig. 6 Equivalent circuit. C_c , capacitance of the concrete; $R_{\text{pore sol}}$, pore solution resistance; C_{dl} , double layer capacitance at the pore solution-electrode interface; R_{ct} , charge transfer resistance of the electrode circuit

the occurrence of the high frequency semi-circle. After 3 days of hydration, the concentration of ions, the porosity and pore size decreases with increasing hydration time leading to an increase in the diameter of the circle [4]. It is reported [14] that between 10 kHz–100 Hz, the resistive loop is mainly due to the cement/electrode interface contribution and in the frequency region <100 Hz, the resistive loop is mainly due to electrode impedance and in the frequency region >100 kHz, the resistive loop is mainly due to the dielectric properties of the concrete [15, 16]. The experimental results have confirmed that

the resistive loop between 100 kHz–100 Hz region is more appropriate for determining ‘D’ in concrete.

Diaz et al. [6] reported that if only the diffusion coefficient is required, a single frequency measurement at 1 kHz will be enough, provided that the driven electrodes are close enough to minimize the electrolyte resistance. In the present work the driven electrodes are spaced at 1 cm intervals and hence this frequency region has been more appropriate for determining the resistance. In concrete, to arrive at the diffusion coefficient from conductivity, both Nernst–Einstein equation and Einstein–Smoluchowski equation have been used [8, 17]. Since the ionic mobility of Na^+ and Cl^- is not established experimentally for the given concentration, the Nernst–Einstein equation has been used in the present study.

3.2 OPC Vs PPC: effect of curing time and strength

Results are summarized in Table 3. M25-OPC when cured for 3 days shows a D_R value of $5.76 \times 10^{-7} \text{ cm}^2/\text{sec}$ and this value gets decreased with an increase in curing time. At the end of 28 days the D_R value is about $1 \times 10^{-7} \text{ cm}^2/\text{sec}$ i.e., nearly 16.7 % of that obtained at the end of 3 days curing. M30-OPC when cured for 3 days shows a D_R value of $2.67 \times 10^{-7} \text{ cm}^2/\text{s}$, which is less than half the value obtained from M25-OPC. This value decreased with an increase in curing time. At the end of 28 days, the D_R value is $0.84 \times 10^{-7} \text{ cm}^2/\text{sec}$ i.e., nearly 33.3 % of that obtained at the end of 3 days curing.

M25-PPC concrete, when cured for 3 days, shows a D_R value of $5.8876 \times 10^{-7} \text{ cm}^2/\text{sec}$ and this value gets decreased with an increase in curing time. At the end of 28 days, the D_R value is about 12.5% of that obtained at the end of 3 days of curing. Similarly in M30-PPC concrete the D_R value at the end of 28 days curing is $0.5276 \times 10^{-7} \text{ cm}^2/\text{sec}$, which is 16.7% of that obtained at the end of 3 days of curing.

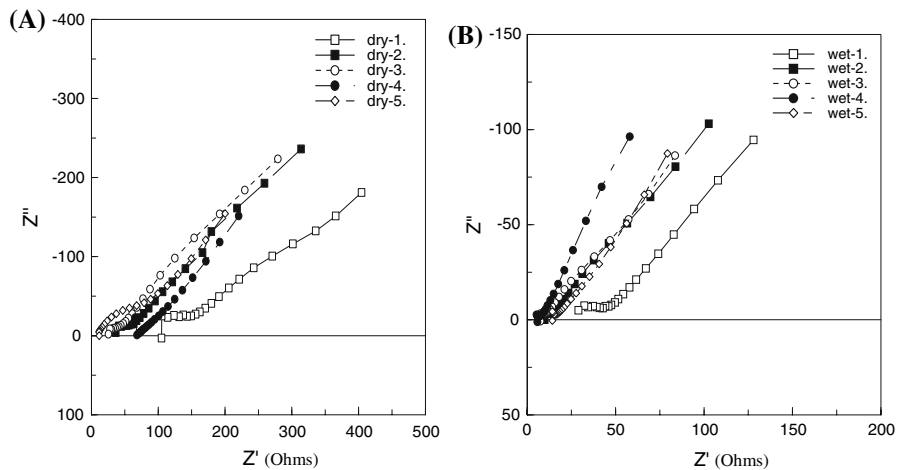
3.3 Effect of alternate wet and dry cycle on resistance

The Nyquist behaviour of M25 and M30 OPC concrete under dry and wet cycle is given in Figs. 7 and 8. It is seen that with time the slope of the low

Table 3 Comparison of D_R : OPC vs PPC concrete

Grade	Curing (days)	OPC			PPC		
		Resistance (Ω)	Conductivity ($\times 10^{-3}$ S/m)	$D_R \times 10^{-7}(\text{cm}^2/\text{s})$	Resistance (Ω)	Conductivity ($\times 10^{-3}$ S/m)	$D_R \times 10^{-7}(\text{cm}^2/\text{s})$
M25	3	39.01	160.2	5.76	38.23	163.5	5.88
	7	60.46	103.4	3.72	102.38	61.05	2.19
	14	180.29	34.7	1.25	185.62	33.7	1.21
	28	221.18	28.3	1.02	311.15	20.1	0.72
M30	3	84.07	74.3	2.67	70.34	88.9	3.19
	7	101.05	61.9	2.23	136.7	45.7	1.64
	14	232.57	26.9	0.97	252.83	24.7	0.89
	28	266.19	24.8	0.84	434.76	14.4	0.52

Fig. 7 Impedance data obtained on M25-OPC concrete: (a) Dry cycle and (b)Wet Cycle



frequency arc slowly reduces and reaches to -1 which indicates the presence of Warburg impedance. The diameter of the high frequency arc also reduces slowly at each cycle indicating the permeation of chloride. The resistance of the concrete is greater under dry cycle than under wet cycle (Table 4). At the end of the 2nd dry cycle, the value of resistance is 142.46 ohms in M25 concrete whereas it is 272.11 ohms in M30 concrete. During drying of concrete, crystallization of chloride in the pores and loss of liquid connectivity inside the porous net work due to moisture loss might have increased the resistance value in the dry cycle [18]. But at the end of 4th dry cycle, resistance decreases to a very low value. This indicates that the crystallized salt in the pores gets dissolved with time leading to an increase of its concentration in the pore solution and a consequently in resistance. Under the wet cycle, the

values are 36.61, 40.74 ohms in M25 and M30 concrete respectively. The data indicates that all the pores are filled with the chloride ion, moisture and thus capillary paths by interconnected pores are established continuously. Due to this the resistance is decreased. From this it is inferred that the moisture movement greatly influences the resistance measurements. The average D_R of M25 and M30 concrete under wet cycle is 6.61×10^{-7} and $5.85 \times 10^{-7} \text{ cm}^2/\text{sec}$ respectively.

3.4 D_p from porosity

From Table 5, it can be seen that porosity decreases with the increase of curing. The porosity is less in PPC concrete compared to OPC concrete. At the end of 28 days of curing, it is 35% and 38% in 25 MPa- whereas it is 34% and 37% in 30 MPa- PPC and OPC



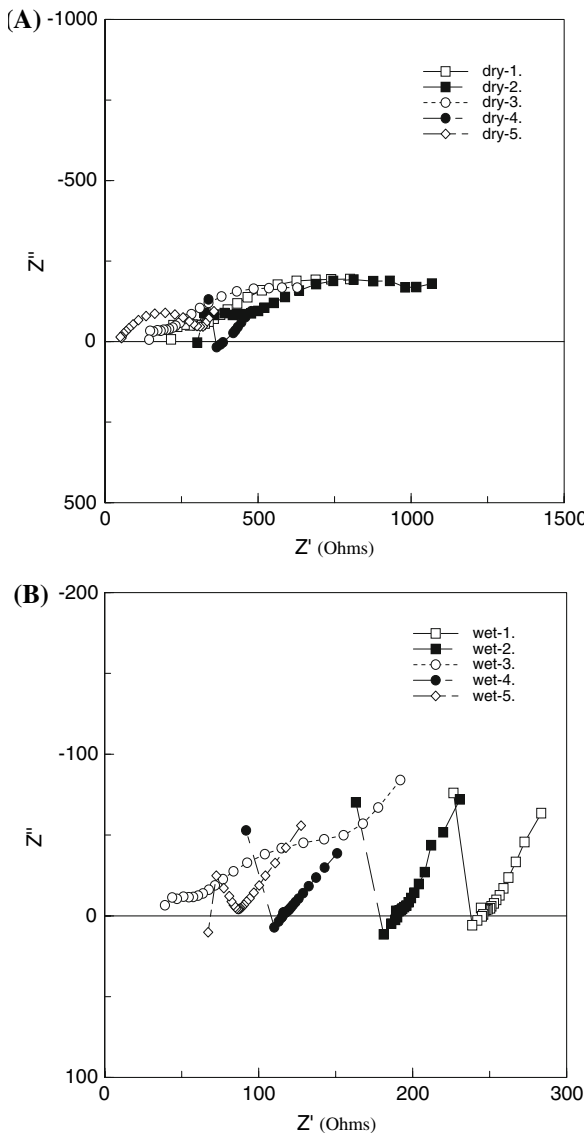


Fig. 8 Impedance data obtained on M30-OPC concrete: (a) Dry cycle and (b) Wet Cycle

concrete respectively. The interfacial zone and percolation effects by the presence of coarse aggregate in the concrete might have increased the porosity. Total porosity of concrete has been correlated with the diffusion co-efficient determined from the resistance (28 days) and this is shown in Fig. 9. The diffusion coefficient having a relation with porosity as:

$$D_p = (0.114P - 3.381) \times 10^{-7}$$

where, P, porosity %; D_p , diffusion coefficient from porosity; cm^2/sec .



As the penetration of chloride through the concrete is a diffusion process without pressure, the porosity of the concrete is usually consistent with the diffusivity of the concrete.

3.5 $D_c(x)$ from chloride concentration

From Table 6, it is clear that, after 64 days of exposure in 0.513 M NaCl solution, the $D_c(x)$ value is $6.24 \times 10^{-7} \text{ cm}^2/\text{s}$ and $5.34 \times 10^{-7} \text{ cm}^2/\text{s}$ in M25 and M30-OPC concrete respectively. The value is very close to the value determined by D_R .

4 Discussion

From Table 3, it can be observed that in PPC concrete, the D_R is higher at the end of 3 days than OPC concrete but at the end of 28 days it is less than the OPC concrete. The densification of pore structure refinement in PPC concrete reduces the pore size. Using resistance measured from EIS, the average pore diameter of the OPC and PPC concrete are calculated as follows; [3]

$$R = \frac{2L}{3S} \frac{\delta}{\sigma_f} \left(\frac{1}{P \times r_0} \right) \quad (7)$$

$$r_0 = \frac{k}{P \times R}$$

where R, resistance (ohms); L, length of the specimen (m); S, surface area (m^2); δ , double layer thickness (m); σ_f , specific conductivity of the pore solution ($\text{Ohm}^{-1} \text{ m}^{-1}$); r_0 , pore diameter (m); P, total porosity (%; v/v); K, constant. From Eq. 7, it can be understood that for determining the pore size, estimation of pore solution conductivity (σ_f) and double layer thickness (δ) is necessary.

4.1 Estimation of specific conductivity of the pore solution

Based on the earlier work carried out by Snyder et al and Larbi et al. [19, 20] on cement paste and mortar, the specific conductivity of the pore solution in the present investigation can be calculated as follows;

Table 4 Comparison of D_R : dry cycle vs wet cycle

Grade	No. of cycle	Dry cycle		Wet cycle	
		Resistance (Ω)	$D_R \times 10^{-7}$ (cm^2/sec)	Resistance (Ω)	$D_R \times 10^{-7}$
M25	1	64.77	5.02	61.9	5.22
	2	142.46	2.29	59.34	5.45
	3	74.07	4.41	46.73	6.92
	4	37.02	8.82	36.61	8.84
	Average		5.13	Average	6.61
M30	1	159.37	2.03	67.46	4.79
	2	272.11	1.19	78.05	4.14
	3	150.16	2.16	49.60	6.52
	4	114.79	2.82	40.74	7.94
	Average		2.05	Average	5.85

Table 5 Comparison of porosity and pore size: OPC vs PPC

Grade	Curing (days)	OPC				PPC			
		K ($\Omega\text{-m}$)	P (% v/v)	R (Ω)	r_0 (μm)	K ($\Omega\text{-m}$)	P (% v/v)	R (Ω)	r_0 (μm)
M25	3	16.90	40.70	39.01	1.062	16.90	39.84	38.23	1.109
	7	16.90	39.49	60.46	0.700	16.90	38.33	102.38	0.431
	14	16.90	38.90	180.29	0.241	16.90	36.90	185.62	0.247
	28	16.90	38.67	221.18	0.198	16.90	35.46	311.15	0.153
M30	3	19.686	40.58	84.07	0.573	19.686	38.61	70.34	0.725
	7	19.686	39.05	101.05	0.499	19.686	37.62	136.70	0.383
	14	19.686	38.65	232.57	0.219	19.686	36.83	252.83	0.211
	28	19.686	37.13	266.19	0.199	19.686	34.61	434.76	0.131

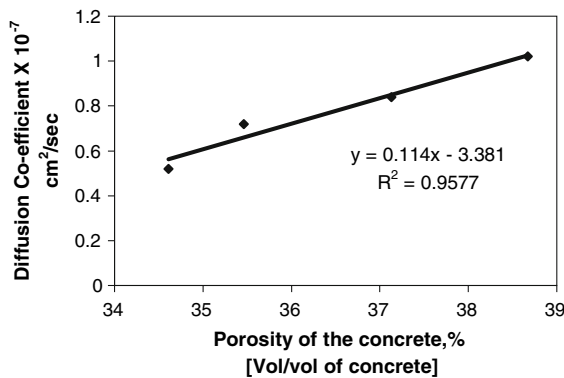


Fig. 9 Correlation between porosity and diffusion coefficient determined from resistance (28 days of Curing)

$$\sigma_f = \sigma_{water} + \sum_i c_i \lambda_i \tag{8}$$

where σ_{water} , specific conductivity of water = $1 \times 10^{-5} \text{ m}^{-1} \Omega^{-1}$; c_i , concentration of the i th ion; λ_i , equivalent conductivity of the i th ion.

Taking into account the equivalent conductivity of ions such as OH^- , K^+ , Na^+ and Cl^- and their molar concentration, conductivity of the pore solution was calculated as $0.0213 \text{ m}^{-1} \Omega^{-1}$.

4.2 Estimation of double layer thickness

Double layer thickness can be arrived at by using the relationship given by Adams [21]

$$\delta = \frac{1}{\kappa} \tag{9}$$

where,

$$\kappa^2 = \frac{4\pi e^2}{\epsilon kT} \sum_i n_i z_i^2 \tag{10}$$

e , charge on the electron ($1.602 \times 10^{-19} \text{ C}$); ϵ , dielectric constant of the cement paste (For M25: 5.58; M30 : 7.58; Reproduced from Ref. [14]);



Table 6 Comparison of diffusion coefficient: D_R vs $D_c(x)$

Grade	Diffusion co-efficient of chloride $\times 10^{-7}$ (cm ² /s)		
	D_R		$D_c(x)$
	Dry cycle	Wet cycle	
M25	5.13	6.61	6.24
M30	2.05	5.85	5.34

k, Boltzman constant (1.38×10^{-23} J K⁻¹); T, temperature in K; n_i , concentration of ith ion (mol/volume); z_i , valence of the ith ion.

Using Eqs. 9 and 10, δ was calculated as 8.597×10^{-6} μm for M25 concrete and 10.016×10^{-6} μm for M30 concrete. By substituting the values of δ and σ_f in Eq. 8, the K value was calculated, which is 16.90 for M25 concrete and 19.686 for M30 concrete. From this K value, by substituting the porosity and resistance, the pore size (r_0) was calculated and given in Table 5.

4.3 Pore size: OPC Vs PPC

Table 5 summarizes the data on porosity 'P', resistance 'R' and pore diameter r_0 with respect to curing time. It can be seen that M25-OPC concrete when cured for 3 days shows a r_0 value of 1.062 μm and this value decreased with an increase in curing time. At the end of 28 days, the r_0 value is 0.198 μm , which is nearly 20% of that, obtained at the end of 3 days of curing. M30-OPC concrete when cured for 3 days shows a r_0 value of 0.573 μm , which is approximately 50% of the value obtained for M25-OPC. This value decreased with an increase in curing time. At the end of 28 days, the r_0 value is 0.199 μm , which is approximately 30% of that, obtained at the end of 3 days of curing.

It is also evident that, compared to OPC concrete, in PPC concrete there is a reduction in pore size at each curing period. M25-PPC concrete having a pore size of 1.109 μm at the end of 3 days and this decreased with an increase in curing time. At the end of 28 days the r_0 value is 0.153 μm which is about 14.3% of that obtained at the end of 3 days curing. In M30-PPC concrete at the end of 3 days curing, the pore size is 0.725 μm , it reached a value of 0.131 μm at the end of 28 days of curing. Higher cement content and lower w/c ratio reduces the pore diameter

in M30 concrete compared to M25 concrete. The pore diameter determined is not the average diameter of the individual pores but it may be the diameter of the largest fraction of the interconnected pores. It was reported that the lower diameter limit of capillary pore size in concrete is normally in the range of 10 nm–100 μm [22, 23]. As shown in the table, at the end of 28 days of curing, the size of all the pores falls in the range between 10 nm to 100 μm , inferences that they are only capillary pores.

Figure 10a shows the plot of pore size with curing time for M25 concrete while Fig. 10b shows the plot of pore size with curing time for M30 concrete. Initially at the end of 3 days the pore size is more in PPC concrete than in OPC concrete. It appears that, at an early age, fly ash in pozzolana cement serves only as an inert component. However after 3 days, due to pozzolanic reaction, the pore size is reduced more in PPC than in OPC. It is interesting to observe that up to a curing period of 14 days, the rate of reduction of pore size is faster in both OPC and PPC. After 14 days, the pore size gets stabilized in OPC whereas in PPC there is a further reduction in pore size. This is obviously due to the pozzolanic reaction.

4.4 Prediction of time to initiation of corrosion

Using D_R , the time to initiation of corrosion was calculated using Eq. 5. By taking cover of concrete as 40 mm (minimum cover recommended for marine environment) and chloride threshold value for initiation of corrosion at the rebar level (C_x) as 0.4 % chloride by weight of cement, [24] the 't' in days was calculated. The results are given in Table 7. Compared to OPC the time to initiation of corrosion in PPC is increased by a factor of 1.24 in M25 concrete and this initiation time increased by a factor of 1.4 times in M30 concrete.

5 Conclusions

From the present investigation carried out on M25 and M30 grade concretes, the following broad conclusions can be drawn:

1. The D_R of PPC concrete is only 66.7 % of that obtained in OPC concrete. Correspondingly PPC



Fig. 10 Comparison of pore diameter Vs curing time. (a) 25 MPa concrete (b) 30 MPa concrete

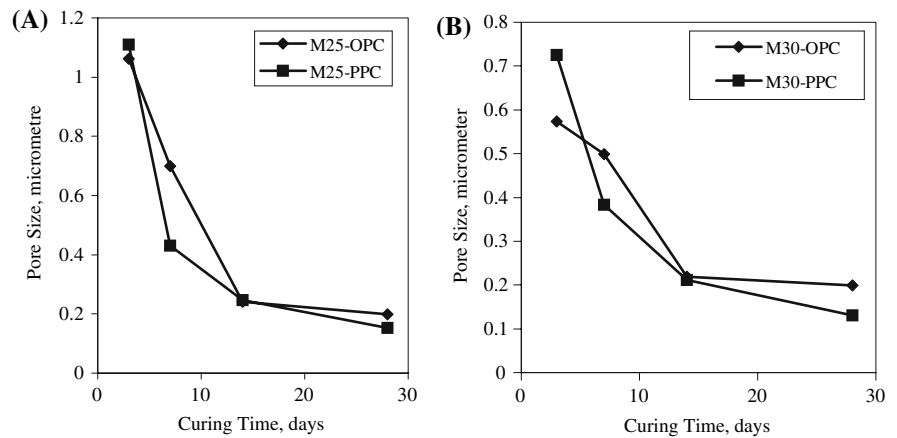


Table 7 Time to initiation of corrosion: OPC vs PPC

Grade of concrete	C_x (Cl^- by weight of cement, %)	C_s (Cl^- by weight of cement, %)	D_R ($\times 10^{-7} \text{cm}^2/\text{sec}$)	x (cm)	Time to initiation of corrosion (days)
M25-OPC	0.4	14.88	1.02	4	187
M25-PPC	0.4	14.88	0.72	4	232
M30-OPC	0.4	12.06	0.84	4	264
M30-PPC	0.4	12.06	0.52	4	375

is more durable than OPC. The lowering of D_R value in PPC concrete is attributed to higher SiO_2 content, densification of pore structure and a reduction in OH^- ion concentration due to pozzolanic reaction.

- At the end of 28 days of curing, D_R of the concrete linearly increases with the total porosity of concrete (expressed in %). This is irrespective of the type of cement used (OPC or PPC) and the strength of the concrete (M25 or M30). Obviously the pores are interconnected.
- The splash zone condition has an important bearing on the D_R values and consequently on the service life. D_R of M30 concrete under the wetting cycle is nearly 3 times that obtained under drying cycle. This indicates that chloride induced corrosion in the splash condition in OPC concrete can initiate in 30 % of as fast of the initiation time of PPC concrete.
- There is a very good correlation between the D_R value obtained under wet cycle and $D_c(x)$ obtained through destructive titration method.
- As the rate of pore refinement is faster in PPC concrete, the reduction of pore size is greater in

PPC concrete than in OPC concrete. The results also indicate that the beneficial effect of PPC concrete by pozzolanic reaction, needs a minimum curing period of 14 days to produce an enhanced durability.

- The time to initiation of corrosion increased considerably, by a factor of 1.2 times of, in M25-PPC concrete compared to OPC concrete and by a factor of 1.4 times of, in M30-PPC concrete.

References

- Cook DJ, Hinczak I, Jedy M, Cao HT (1989) Proceedings of 3rd International Conference on Fly Ash, Silica Fume, Slag and Natural Pozzolana in Concrete. ACI SP-114 1467–1483
- Xu Z, Ping Gu, Ping Xie, Beaudoin JJ (1993) Application of A.C. Impedance techniques in studies of porous cementations materials (II): relationship between ACIS behavior and the porous microstructure. *Cem Con Res* 23:853–862
- Beaudoin JJ, Tamtsia BT (2004) Creep of Hardened Cement Paste—The Role of Interfacial Phenomena. *Inter Sci* 12:353–360
- Poupard O, Ait-Mokhtar A, Dumargue P (2004) Corrosion by chlorides in reinforced concrete: Determination of

- chloride concentration threshold by impedance spectroscopy. *Cem Con Res* 34:991–1000
5. Buchwald A (2000) 'Determination of the ion diffusion coefficient in moisture and salt loaded masonry materials by impedance spectroscopy' 3rd Int. PhD Symposium 11–13. Oct 2000, Vienna, vol 2, p 475
 6. Diaz B, Novoa XR Perez MC (2006) Study of the chloride diffusion in mortar: A new method of determining diffusion coefficients based on impedance measurements. *Cem Con Res* 28:237–245
 7. McCarter WJ, Brousseau R (1990) The A.C. response of hardened cement paste. *Cem Con Res* 20(6):891–900
 8. Lu X (1997) Application of the Nernst-Einstein equation to concrete. *Cem Con Res* 27(2):293–302
 9. Standard test method for specific gravity, absorption and voids in hardened concrete (1995) ASTM C642–80, ASTM, USA
 10. I.S. 4031(1988) 1988 Method of physical tests for hydraulic cement: bureau of Indian standards, NewDelhi
 11. Muralidharan S, Vedalakshmi R, Saraswathy V, Palaniswamy N (2005) Studies on the aspects of chloride ion determination in different types of concrete under macro-cell conditions. *Build Environ* 40(9):1275–1281
 12. Browne RD (1980) Mechanism of corrosion of steel in concrete in relation to design, inspection, and repair of offshore and coastal structures. Performance of concrete in marine environment, ACI SP -65 pp 169–204
 13. Maekawa K, Ishida T, Kishi T (2003) Multi scale modeling of concrete performance Integrated material and structural Mechanics. *Adv Con Technol* 1:91–126
 14. Cabeza M, Merino P, Mirinda A, Novoa XR, Sanchez I (2002) Impedance spectroscopy study of hardened Portland cement pastes. *Cem Con Res* 32:881–891
 15. Andrade C, Blanco VM, Collazo A, Keddad M, Rnovo X, Takenouti H (1999) Cement paste hardening process studied by Impedance spectroscopy. *Electrochim Acta* 44:4313–4318
 16. Bard AJ, Faulkner IR (2001) *Electro chemical methods: Fundamentals and applications* 2nd edn. John Wiley and Sons, pp 139–145
 17. Keddad M, Takenouti H, Novoa XR, Andrade C, Alonso C (1997) Impedance measurements on cement pastes. *Cem Con Res* 27(8):1191–1201
 18. Liu Z, Beaudoin JJ (1999) An assessment of the relative permeability of cement system using AC impedance techniques. *Cem Con Res* 29:1085–1090
 19. Snyder KA, Feng X, Keen BD, Mason TO (2003) Estimating the electrical conductivity of cement paste solutions from OH^- , K^+ and Na^+ concentrations. *Cem Con Res* 33:793–798
 20. Larbi JA, Visser JH (2002) A study of the ASR of an aggregate with high chert content by means of ultra-accelerated mortar bar test and pore fluid analysis. *HERON* 47(2):141–159
 21. Adamson AW (1982) *Physical chemistry of surfaces*. John Wiley and sons, 4th edn. pp 185–195
 22. Roy DM, Brown PW, Shi S, Scheetz BE, May W (1993) Concrete microstructure, porosity and permeability. *SHRP-C* 628:44–46
 23. Pivinka P, Hellmich C, Smith D (2004) Microscopic effects on chloride diffusivity of cement pastes- A scale transition analysis. *Cem Con Res* 34:2251–2260
 24. ACI 318 Building code requirements for reinforced concrete (1989) American Concrete Institute, Michigan